Published in final edited form as:
J Biol Chem. 2006 December 22; 281(51): 39033. doi:10.1074/jbc.M605097200.

Control of Death-associated Protein Kinase (DAPK) Activity by Phosphorylation and Proteasomal Degradation*

Yijun Jin‡, **Emily K. Blue**§, and **Patricia J. Gallagher**[1,§]

‡ Department of Molecular and Cellular Physiology, Louisiana State University Health Science Center, Shreveport, Louisiana 71103

§ Department of Cellular and Integrated Physiology, Indiana University School of Medicine, Indianapolis, Indiana 46202

Abstract

Activation of death-associated protein kinase (DAPK) occurs via dephosphorylation of Ser-308 and subsequent association of calcium/calmodulin. In this study, we confirmed the existence of the alternatively spliced human DAPK-*β*, and we examined the levels of DAPK autophosphorylation and DAPK catalytic activity in response to tumor necrosis factor or ceramide. It was found that DAPK is rapidly dephosphorylated in response to tumor necrosis factor or ceramide and then subsequently degraded via proteasome activity. Dephosphorylation and activation of DAPK are shown to temporally precede its subsequent degradation. This results in an initial increase in kinase activity followed by a decrease in DAPK expression and activity. The decline in DAPK expression is paralleled with increased caspase activity and cell apoptosis. These results suggest that the apoptosis regulatory activities mediated by DAPK are controlled both by phosphorylation status and protein stability.

Apoptosis is a highly coordinated cellular process that serves to eliminate unwanted cells. Because of its fundamental role in maintaining the integrity of multicellular organisms, it is not surprising that apoptosis is tightly regulated by a multitude of signaling proteins, including death-associated protein kinase (DAPK)[2] (1). DAPK has been implicated in regulating apoptosis induced by a variety of stimuli, including tumor necrosis factor (TNF) and ceramide as well as oncogenes such as c-*Myc* and p53 (2–7). Depending on the particular cell type, the response to specific apoptosis inducers can vary, and DAPK can either promote (3–5,8) or antagonize apoptosis (2,7). Regardless of the apoptotic outcome, the effects of DAPK are dependent upon its catalytic activity as well as by its interaction with other proteins through its noncatalytic domains (2,9–13).

The kinase domain of DAPK has a high homology to the kinase domain of smooth muscle myosin light chain kinase and as expected can also phosphorylate the regulatory light chain

*This work was supported by National Institutes of Health Grant NHLBI HL54118 (to P. J. G.), American Heart Association Scientist Development Grant 0435064N (to Y. J.), and Indiana University Diabetes and Obesity Research Training Grant DK064466 (to E. K. B.).

1To whom correspondence should be addressed: Dept. of Cellular and Integrated Physiology, Indiana University School of Medicine, 635 Barnhill Dr., Indianapolis, IN 46202-5120; Tel.: 317-278-2146; Fax: 317-274-3318; pgallag@iupui.edu.

The nucleotide sequence(s) reported in this paper has been submitted to the Gen-Bank™/EBI Data Bank with accession number(s) EF090258.

2The abbreviations used are: DAPK, death-associated protein kinase; DIP1/MIB1, DAPK-interacting protein1/mindbomb1; TNF, tumor necrosis factor; CHX, cycloheximide; RLC, myosin II regulatory light chain; Ca^{2+}/CaM, calcium/calmodulin; AP, alkaline phosphatase; PARP, poly(ADP-ribose) polymerase; Hu, human; *p*NA, *p*-nitroanilide; CHAPS, 3-[(3-cholamidopropyl)di-methylammonio]-1-propanesulfonic acid; RT, reverse transcription; GFP, green fluorescent protein; E3, ubiquitin-protein isopeptide ligase.

(RLC) of myosin II. Studies have confirmed that a conserved lysine residue within the catalytic site is important for ATP binding, and mutation of this lysine (K42W or K42A) abolishes the effect of DAPK on apoptosis (2,9). The catalytic activity of DAPK is regulated by Ca^{2+}/CaM and by autophosphorylation of Ser-308 within the Ca^{2+}/CaM binding domain. Similar to myosin light chain kinase, phosphorylation of this site inhibits Ca^{2+}/CaM binding and provides a mechanism that negatively regulates DAPK activity (14–16).

DAPK has been shown to interact with DIP1/MIB1 (DAPK-interacting protein-1/mind-bomb) primarily through the ankyrin repeats domain of DAPK (17,18). DIP1/MIB1 is an E3 ligase, and among its multiple functions, it mediates the poly-ubiquitination and proteasomal degradation of DAPK (17) and the mono-ubiquitination of Delta ligand in the Notch signaling pathway (18). This finding raises the possibility that controlling DAPK stability may be a mechanism to regulate the protein levels of DAPK and hence its overall activity. Consistent with this proposal is a recent study demonstrating that HSP90 binds to and stabilizes DAPK, providing another pathway to regulate the activities of this complex kinase (19). Ubiquitination and subsequent proteasomal degradation are common mechanisms for controlling the level of proteins involved in regulating apoptosis, such as caspases and inhibitors of caspases. It has been reported that the expression of DAPK is lost in some types of cancer by promoter hypermethylation, although the significance of down-regulating DAPK expression in the transition of these normal cells to transformed cells is uncertain when the dual pro- and anti-apoptotic functions of this kinase are considered (20–27). In this study, we determined whether the expression level of DAPK is acutely altered during TNF- or ceramide-induced apoptosis and whether ubiquitination and proteasomal degradation are responsible for the change in DAPK protein levels.

One important aspect of DAPK functionality that has not been extensively pursued is the relationship between activation of DAPK and the stability of the protein in response to apoptotic stimuli (17). In this study, we examined the kinase activity of DAPK during TNF- or ceramide-induced apoptosis, and its relationship to DAPK Ser-308 phosphorylation and total DAPK protein levels. We found that DAPK activities, which are critical in determining the progression of TNF- or ceramide-induced apoptosis (3–5,8), are modulated both by autophosphorylation of Ser-308 and by proteasomal degradation. These studies reveal that alterations in DAPK stability in addition to changes in its kinase activity occur in response to these stimuli. These alterations occur in a temporally distinct pattern during the progression of apoptosis, and it is likely that the balance of these activities ultimately determines the pro- or anti-apoptotic outcome. Thus, when phosphorylation of Ser-308 is low, survival predominates, and when proteasomal degradation is increased to deplete cellular levels of DAPK, apoptosis ensues.

MATERIALS AND METHODS

Cells, Antibodies, and Reagents

HeLa cells are from the ATCC (Manassas, VA). HeLa cells expressing tetracycline-inducible mouse DAPK-α or DAPK-β were created and maintained in this laboratory as described previously (2). Antibodies to DAPK (clone DAPK-55) and DAPK phosphorylated on Ser-308 (clone DKPS308) were purchased from Sigma. Antibodies to poly(ADP-ribose) polymerase (PARP) were obtained from Santa Cruz Biotechnology (Santa Cruz, CA). Human tumor necrosis factor-α (TNF) and cycloheximide (CHX) were purchased from Calbiochem. The proteasome inhibitor, MG-132, and *N*-hexanoyl-D-sphingosine (C_6-ceramide) were from Sigma.

RT-PCR Detection of Human DAPK-β

First Choice RACE-ready cDNA from human brain was purchased from Ambion. Total RNA from human coronary artery smooth muscle primary cells (Cell Applications, Inc.) was prepared using Trizol according to the manufacturer's instructions (Invitrogen), and cDNA synthesis was performed in a mixture containing 400 ng of total RNA, random primers, and reverse transcriptase (Invitrogen). For RT-PCR detection of DAPK-α and DAPK-β isoform mRNAs, a combination of a sense primer (SP) 5′-TTGCTGAAGGCATCCTCTGTG-3′ (SP1), 5′-TCAGACCTGAACCTCCTCACTCG-3′ (SP2), and an antisense primer (ASP) of 5′-ACAGAGAGGTAGCGTTTCCTTG-3′ (ASP1) was used to generate fragments. The amplification was carried out in a 50-μl mixture containing 1 μl of cDNA, 1 mM each of the sense and antisense primers, 1 unit of Platinum Taq High Fidelity, 1× High Fidelity PCR Buffer, and 0.2 mM dNTPs (Invitrogen). The reaction conditions were as follows: initial denaturation at 94 °C for 2 min and 35–45 cycles of amplification (94 °C for 0.5 min, 55 °C for 0.5 min, and 68 °C for 0.75 min), followed by a final extension step of 10 min at 68 °C. The products were analyzed by agarose gel electrophoresis for size estimation, subcloned into pCR4-TOPO using the TOPO TA cloning kit (Invitrogen), and were sequenced to verify the insert. The nucleotide sequence for the PCR fragment confirming the alternatively spliced human DAPK-β has been deposited in the GenBank™ under accession number EF090258.

Immunoprecipitation and in Vitro Kinase Assay

Endogenous human DAPK or overexpressed mouse mutant (S308A or S308D) DAPK was immunoprecipitated from HeLa cells and subjected to an *in vitro* kinase assay as described previously (2). The amount of phosphorylated RLC was quantified from Western blotting of phospho-RLC using an antibody specific for RLC phosphorylated on Ser-19, purchased from Cell Signaling Technology.

Alkaline Phosphatase Treatment and Calmodulin Overlay Assay

Immunoprecipitated DAPK was washed and incubated with 50 units of calf intestine alkaline phosphatase (AP, New England Biolabs) in a buffer containing 50 mM Tris-HCl, pH 7.4, and 150 mM NaCl for 30 min at room temperature. For calmodulin overlay assay, immunoprecipitated DAPK was Western-blotted and incubated with biotinylated calmodulin (CaM, Sigma) in a buffer containing 50 mM Tris-HCl, pH 7.4, 150 mM NaCl, 1 mM Ca^{2+} and 5% nonfat dry milk. Calmodulin was detected with streptavidin-conjugated horseradish peroxidase (The Jackson Laboratory).

Caspase Activity Assay

Caspase assays utilize specific caspase substrates Ac-IETD-*p*NA (caspase-8), Ac-DEVD-*p*NA (caspase-3), or Ac-LEHD-*p*NA (caspase-9) (7). For measurement of caspase activity *in vivo*, both adherent and floating cells were collected and lysed with CHAPS lysis buffer (0.1% CHAPS, 100 mM NaCl, 100 μM EDTA, 10 mM dithiothreitol, and 50 mM HEPES, pH 7.4). For every cell sample, nonspecific background was determined by adding the caspase inhibitors, acetyl-IETD-aldehyde (Ac-IETD-CHO; caspase-8), acetyl-DEVD-aldehyde (Ac-DEVD-CHO; caspase-3), or acetyl-LEHD-aldehyde (Ac-LEHD-CHO; caspase-9) as negative control.

Cell Death Assay

Quantification of apoptotic cell death was performed as described previously (2). Briefly, after 4 h of treatment with TNF (10 ng/ml) and CHX (10 μg/ml), cells were fixed and stained for LacZ expression. Apoptotic cells with membrane blebbing were identified morphologically and counted. The extent of apoptosis is defined as follows: (the number of blue apoptotic cells)/(the total number of blue cells).

Data Analysis

All experiments were independently performed at least three times. All statistic analysis and graphs were created using GraphPad Prism software (GraphPad Software, San Diego). Phospho-DAPK level is normalized to the level of total DAPK in Fig. 2*C*. Western blotting data were quantified by densitometry and are representative of at least three repeated experiments.

RESULTS

Dephosphorylation of Ser-308 in DAPK Enhances Kinase Activity

DAPK is phosphorylated on several residues, including an autophosphorylation site at Ser-308 (14). Mutation of Ser-308 to alanine increases the Ca^{2+}/CaM-dependent kinase activity of DAPK (14). In this study, we investigated whether dephosphorylation of Ser-308 of the endogenous DAPK was capable of increasing DAPK activity. Initially, the basal level of human DAPK autophosphorylated at Ser-308 (phospho-DAPK) in HeLa cells was determined by immunoprecipitation utilizing an antibody specific for DAPK phosphorylated at Ser-308. The relative levels of phospho-DAPK and nonphosphorylated DAPK were detected and quantified following Western blotting of the immunoprecipitate and the immunoprecipitation supernatant (Fig. 1*A*). This analysis showed that the relative levels of immunoprecipitated phospho-DAPK and nonphosphorylated DAPK remaining in the post-immunoprecipitation supernatant are approximately equal, suggesting that about 50% of human DAPK is autophosphorylated on Ser-308 under basal conditions.

In vitro treatment of immunoprecipitated total human DAPK with alkaline phosphatase (AP) significantly reduced the level of phospho-DAPK (Fig. 1*B*). The AP-treated, dephosphorylated DAPK bound Ca^{2+}/CaM with higher affinity (Fig. 1*B*). The kinase activities of both the AP-treated and untreated DAPK were measured using purified myosin II RLC as a substrate in an *in vitro* kinase assay as described previously (2). After the reaction was stopped, the phosphorylated RLC was analyzed by Western blotting using an antibody specific for RLC phosphorylated on Ser-19 and quantified by densitometry. Because DAPK is only partially activated by Ca^{2+}/CaM binding, the kinase assays were performed both in the presence or absence of Ca^{2+}/CaM. These results show that the Ca^{2+}/CaM-independent kinase activity of AP-treated human DAPK is 5-fold higher than untreated DAPK (Fig. 1*C*). This is consistent with the previous report that ablation of Ser-308 autophosphorylation increases Ca^{2+}/CaM-independent kinase activity (14). AP-treated DAPK also has 2-fold higher Ca^{2+}/CaM-dependent kinase activity than untreated DAPK (Fig. 1*C*).

DAPK Expression and Activity Decrease following Dephosphorylation during TNF- and Ceramide-induced Apoptosis

DAPK has an important kinase-dependent role in regulating TNF- or ceramide-induced apoptosis (3,5,9,14). We thus examined levels of the endogenous human DAPK activity in HeLa cells treated with TNF (10 ng/ml) and CHX (10 μg/ml) or CHX alone (data not shown) for up to 6 h, or with C_6-ceramide (50 μM) for up to 32 h. Endogenous DAPK was immunoprecipitated, and its kinase activity was determined by an *in vitro* kinase assay with myosin II RLC as substrate. Phospho-RLC was detected with a specific antibody that detects phosphorylation of Ser-19 and quantified by densitometric scanning (Fig. 2*A*). Although the kinase assays were performed both in the presence or absence of Ca^{2+}/CaM, only results from assays conducted in the presence of Ca^{2+}/CaM are shown as both Ca^{2+}/CaM-dependent and -independent kinase activities of DAPK had similar changes in the magnitude of the response to TNF. These results demonstrate that DAPK kinase activity increases between 15 and 30 min in response to TNF treatment, reaching 3-fold higher than the initial level by 60 min. After 60 min, DAPK activity drops dramatically, dipping below the initial level of kinase activity at

120 min and having only 50% of the initial kinase activity left after 6 h of TNF/CHX treatment. DAPK activities in HeLa cells treated with C_6-ceramide for up to 32 h have similar biphasic profiles, in which DAPK kinase activity gradually increases to greater than 2-fold of the basal level by 8 h and thereafter declines to basal level.

To determine the relationship between DAPK activity and DAPK autophosphorylation, protein levels of phospho-DAPK as well as total DAPK were analyzed by Western blotting (Fig. 2, *B* and *C*). Expression of phospho-DAPK begins to decline beginning between 15 and 30 min of TNF/CHX treatment or following 2 h of ceramide treatment. Total levels of DAPK also decrease, although this is not detectable until after 2 h of TNF/CHX treatment or after of 16 h of ceramide. Normalization of phospho-DAPK level to the total DAPK level revealed that TNF treatment induces a rapid and sustained dephosphorylation of DAPK at Ser-308. After 60 min of TNF/CHX treatment (Fig. 2, *B* and *C*), the level of phosphorylation is only 20% that of nontreated cells. Because it was determined that 50% of the total DAPK in nontreated cells is autophosphorylated (Fig. 1*A*), then by extrapolation, in the TNF/CHX cells only 10% of total DAPK will be autophosphorylated after 60 min. A similar decrease in phosphorylation of DAPK at Ser-308 is also detected after 8 h of C_6-ceramide treatment (Fig. 2, *B* and *C*). Together these data define the temporal succession of events that begin with dephosphorylation of Ser-308 to result in increased catalytic activity and the subsequent decline in activity, which results from the decrease in DAPK expression.

In parallel experiments, caspase-9 activity in HeLa cells treated with TNF/CHX or ceramide was determined by a colorimetric assay using a caspase-9-specific substrate. The temporal increase in caspase-9 activity is delayed, and an increase over the basal levels is not detectable until after 60 min of TNF/CHX treatment or 8 h of ceramide treatment. (Fig. 2*C*). Interestingly, the increase in caspase-9 activity is delayed until after a significant decline in DAPK kinase activity occurs raising the possibility that there is an inverse relationship between these activities.

A Mutant, Unphosphorylatable DAPK (DAPK-S308A), Protects Cells from TNF- or Ceramide-induced Apoptosis

The above results suggest that in response to TNF or ceramide, DAPK is initially dephosphorylated and activated, perhaps to antagonize and attenuate the apoptotic signaling of TNF or ceramide. If this is true, then overexpression of a mutant DAPK lacking the autophosphorylation site (DAPK-S308A) should protect cells from TNF- or ceramide-induced apoptosis. To test this, we expressed mutant unphosphorylatable mouse DAPK-S308A and DAPK-S308D, a phosphomimetic mutant with a serine to aspartic acid substitution of either DAPK-α or DAPK-β in HeLa cells. As the results of kinase assays from both DAPK-α and DAPK-β mutants are indistinguishable, only the results for mouse DAPK-α are shown in Fig. 3, *A* and *B*. As expected, both mutant forms of DAPK are not phosphorylated on Ser-308, as confirmed by the absence of signal using the phos-pho-Ser-308-DAPK-specific antibody (Fig. 3*A*). DAPK-S308D also has a lower affinity for Ca^{2+}/CaM as evidenced by its inability to bind CaM in the presence of Ca^{2+} using a ligand-blotting assay (Fig. 3*A*). This result suggests that mutation of Ser-308 to aspartic acid (S308D) results in a kinase that resembles the Ser-308 autophosphorylated DAPK (Fig. 1*B*).

The kinase activities of these mutant mouse DAPKs were evaluated using an *in vitro* kinase assay with myosin II RLC as substrate (Fig. 3*B*). These assays showed that DAPK-S308A is twice as active as wild type DAPK (DAPK-WT), in the presence or absence of Ca^{2+}/CaM, whereasDAPK-S308D retains less than 20% of the kinase activity of DAPK-WT. These data suggest that when expressed in cells, DAPK-S308D will act as a dominant negative by competing with endogenous DAPK.

Although mouse DAPK-*α* and DAPK-*β* have indistinguishable kinase activities, DAPK-*β* is more potent than DAPK-*α* in protecting HeLa cells from TNF-induced apoptosis (2). To test the effect of DAPK-Ser-308 mutants on TNF-induced apoptosis in HeLa cells, plasmids encoding either wild type or mutant DAPK-*α* or DAPK-*β* S308A or S308D were cotransfected with LacZ into HeLa cells. The transfection efficiency was similar for all the plasmids, as shown by Western blotting of recombinant DAPKs (Fig. 3*C*). After treatment with TNF/CHX for 4 h, cells were fixed and stained for LacZ expression. The percentage of LacZ-positive cells that had obvious apoptotic morphology (blebbing and condensed cytoplasm) was determined to monitor apoptosis (Fig. 3*C*). After 4 h of TNF treatment, 75% of control cells that were transfected with LacZ alone had apoptotic morphology. Cells that were transfected with mouse DAPK had a lower percentage of apoptotic cells, although statistical significance was achieved only for cells expressing DAPK-*β*. Similarly, overexpression of DAPK-*β*-S308A, a mutant mouse DAPK-*β* that has higher kinase activity than wild type DAPK-*β* because of loss of the inactivating autophosphorylation site (Fig. 3*B*), further decreased the level of apoptotic cells to 30%. In contrast, overexpression of an autophosphorylation site mimetic, DAPK-*β*-S308D, a mutant DAPK-*β* that has lower kinase activity than wild type DAPK-*β* (Fig. 3*B*), increased the percentage of apoptotic cells to 90%, suggesting DAPK-*β*-S308D acts as a dominant negative to promote apoptosis. Consistent with our previous studies suggesting that overexpression of DAPK-*α* does not overtly promote apoptosis, but rather acts as a weak survival factor (2), expression of either wild type, S308A, or S308D DAPK-*α* form did not significantly increase or decrease the apoptotic levels of TNF-treated HeLa cells.

Plasmids encoding either wild type or mutant mouse DAPK-*α* or DAPK-*β* S308A or S308D were also cotransfected with GFP into HeLa cells. The GFP-positive cells were enriched by fluorescence-activated cell sorter and were positive for the recombinant DAPKs (Fig. 3*D*). After treatment with C_6-ceramide for 24 h, both the floating and adherent cells were collected and assayed for cellular activities of caspase-3, caspase-8, and caspase-9 (Fig. 3*D*). Although ceramide induces little caspase-8 activity in HeLa cells, the activities of both caspase-9 and caspase-3 increased significantly. Consistent with its role as an anti-apoptosis protein, overexpression of mouse DAPK-*β* decreases both caspase-3 and caspase-9 activities. Increasing DAPK-*β* activity by abolishing the autophosphorylation site (S308A) further reduces caspase-3 or caspase-9 activities. Inhibition of DAPK-*β* activity by mimicking the constant autophosphorylation (S308D), on the contrary, increases caspase-3 and caspase-9 activities to levels more than those of the wild type cells. Again, overexpression of either DAPK-*α* or its Ser-308 mutants did not have a statistically significant effect on ceramide-induced caspase-3 or caspase-9 activities. Together these results suggest that enhancing DAPK-*β* kinase activity by loss of inhibitory autophosphorylation via dephosphorylation of DAPK-*β* Ser-308 suppresses caspase activation, whereas inhibition of DAPK-*β* kinase activity by maintaining phosphorylation of DAPK-*β* Ser-308 enhances caspase activities in HeLa cells treated with ceramide.

Identification of an Alternatively Spliced Human DAPK, DAPK-β

To date, no alternative spliced forms of human DAPK have been identified either by cloning or by examination of data bases. To determine whether an alternatively spliced isoform of human DAPK exists, Western blotting and RT-PCR studies were performed. To detect human DAPK-*β* by Western blotting, as described previously (2), affinity-purified antibody directed against the 12 unique residues (RDSHAWTPLYDL) comprising the carboxyl-terminal extension of the mouse DAPK-*β* was used to examine cell lysates prepared from human and mouse cell lines (Fig. 4*A*). These results show that the mouse anti-DAPK-*β*-specific antibody detects a 150-kDa protein in both human and mouse cell lines. This suggests that similar to mouse DAPK, an alternatively spliced human DAPK-*β* exists that can be recognized by this antibody. Examination of the 3′-untranslated region of the human DAPK identified a potential

alternative splice site that, when translated, was similar in sequence to the 12 residues in mouse DAPK-*β*. To determine whether this corresponded to an alternative splice site, which would generate human DAPK-*β*, RT-PCR was performed on RNA purified from human tissue and primary cell lines. For this, two sets of primers spanning between the known sequence of human DAPK and the potential splice site were synthesized and tested. As shown in Fig. 4*B*, both primer sets generated fragments corresponding to the predicted alternative splice site, confirming the presence of human DAPK-*β*. Sequencing of the PCR fragments confirmed that they correspond to human DAPK and extend its carboxyl terminus by 10 residues, which are nearly identical to mouse DAPK-*β* (Fig. 4*C*).

TNF Induces Proteasomal Degradation of DAPK

The results in Fig. 2 show that as the protein and activity levels of DAPK decrease after 60 min of TNF/CHX treatment, there is a corresponding increase in caspase-9 activity. We next determined whether the stability of the two DAPK isoforms is altered. With regard to this, we have previously identified a DAPK-interacting protein (DIP1/MIB1), which is an E3 ligase that can target DAPK for degradation by addition of poly-ubiquitin both *in vitro* and *in vivo* (17). To determine whether ubiquitination of DAPK is important for regulating its cellular levels in TNF-induced apoptosis and whether both forms of DAPK are equally sensitive to proteasome-mediated degradation, we compared the expression levels of recombinant mouse DAPK-*α* and DAPK-*β* in response to TNF/CHX or CHX alone (Fig. 5*A*). Western blotting to detect either the recombinant mouse DAPK-*α* and DAPK-*β* exogenously expressed in HeLa cells using an anti-Omni tag antibody shows that DAPK-*β* is less stable than DAPK-*α* (Fig. 5*A*), becoming undetectable after 7.5 h of TNF/CHX treatment, whereas the level for DAPK-*α* is ~25% of the initial level. In control experiments, using HeLa cells treated with CHX alone, the levels of both recombinant mouse DAPK-*α* or DAPK-*β* do not change, suggesting that the decline in expression is a specific response to TNF signaling (Fig. 5*A*).

To demonstrate that the endogenous human DAPK, similar to mouse DAPK, is also sensitive to ubiquitin-mediated degradation, we overexpressed the ubiquitin ligase that targets mouse DAPK, DIP1/MIB1 (Fig. 4*B*), and examined the effects on human DAPK stability using Western blotting. Treatment of the HeLa cells with TNF alone (no CHX) resulted in a significant reduction of the expression level of total human DAPK and DAPK-*β* within 4 h (Fig. 5*B*) suggesting that TNF also results in human DAPK degradation. In HeLa cells overexpressing DIP1/MIB1, the relative levels of total human DAPK as well as the human DAPK-*β* isoform are significantly lower than in respective parental HeLa cells either in the presence or absence of TNF. These results suggest that like mouse DAPK (2,17), human DAPK can be targeted for degradation by DIP1/MIB1 and that ubiquitination of DAPK has a role in regulating the cellular levels of DAPK through proteasomal degradation.

To confirm that ubiquitination of DAPK was responsible for promoting the degradation of DAPK, we tested whether MG132, an inhibitor of proteasomal activity, could stabilize DAPK expression. Fig. 5*C* shows that the levels of the endogenous human total DAPK as well as DAPK-*β* expression in TNF-treated HeLa cells are stabilized when the cells are treated with TNF/CHX and MG-132 (50 μM). To assess progression of TNF-induced apoptosis in this experiment, we also examined the cleavage of PARP into an 89-kDa fragment as an indicator of caspase activation (Fig. 5*C*). These results show that treatment of HeLa cells with MG-132 effectively inhibits PARP cleavage induced by TNF, a result consistent with the suggestion that an inverse relationship between caspase activity and DAPK expression levels exists in cells undergoing TNF-induced apoptosis.

DISCUSSION

Although the kinase activity of DAPK has been shown to be important for DAPK to regulate a number of apoptosis pathways, the temporal modulation of its kinase activity in response to apoptotic stimuli is not well characterized. In this study, we used an *in vitro* kinase assay to determine the activity of endogenous human DAPK immunoprecipitated from HeLa cells treated with TNF or ceramide. The kinase activity profile of DAPK is biphasic in response to these apoptotic stimuli with DAPK activity initially increasing as a result of dephosphorylation of the autophosphorylation site, Ser-308. In the second phase, the activity of DAPK declines, and this decline is paralleled by a decrease in DAPK expression and by an increase in caspase-9 activity. Most importantly, these studies also reveal that once Ser-308 is dephosphorylated in response to TNF or ceramide, the catalytic activity of DAPK is not attenuated through re-phosphorylation of Ser-308, as the levels of phospho-DAPK do not increase in parallel with the decline in RLC phosphorylating activity. Rather the mechanism by which the catalytic activity of DAPK is attenuated is by ubiquitination of the kinase, which targets it for degradation by the proteasome.

Our previous studies have shown that the cellular levels of DAPK can be directly regulated by proteasomal degradation and identified a novel DAPK E3 ubiquitin ligase containing three RING fingers called DIP1 (17). DIP1 was shown to mediate poly-ubiquitination of DAPK both *in vitro* and *in vivo*. Subsequently, DIP1 was shown to be identical to mindbomb (MIB1), and these experiments demonstrated that DIP1/MIB1 mono-ubiquitinates Delta-1 to cause its endocytosis as part of the initiation of the Notch signaling pathway (18). Although we cannot conclude that DIP1/MIB1 is the only ubiquitin ligase that has a direct role for regulating the cellular levels of DAPK, these studies have demonstrated that one mechanism for the attenuating DAPK activity is by its degradation via the proteasome. This conclusion is supported by the use of the proteasome inhibitor MG-132, which reverses degradation of human DAPK and in parallel abrogates TNF-induced apoptosis. These results indirectly link the cellular levels of DAPK to the rescue of HeLa cells from TNF-induced apoptosis.

It is not surprising that the temporal sequence of changes in DAPK autophosphorylation levels, catalytic activity, and expression levels in response to ceramide treatment parallels the changes observed for cells exposed to TNF. However, consistent with the known death-promoting effects of ceramide, the time course of these events is more protracted. Ceramide is a second messenger generated by TNF treatment, which also results in activation of non-caspase proteases like cathepsin B (28–30). Ceramides are also phosphatase activators (31–33), which may provide a link to the mechanism by which dephosphorylation of DAPK occurs. Although the exact phosphatase that dephosphorylates DAPK has not been characterized, a recent study found that FK506, a calcineurin inhibitor, can inhibit dephosphorylation of DAPK, raising the possibility that this phosphatase has a role in the activation of DAPK (34).

Although the role of DAPK in TNF signaling is not completely understood, it seems likely that DAPK has a unique and important role in this signaling cascade. In support of this proposal is the recent observation that DAPK associates with tumor necrosis factor receptor 1 and FADD in neuronal cells of rats stimulated to undergo seizure (35). This finding positions DAPK to have an important and direct role in TNF signaling. The TNF signaling pathway has two arms that can result in promoting apoptosis or alternatively promoting cell growth/proliferation. Our data suggest that activated DAPK may serve as a “checkpoint” or braking protein by opposing apoptosis. The initial increase in DAPK activity in response to TNF treatment could function as a cytoprotective mechanism that requires activation of DAPK to counter the apoptotic arm of the TNF signaling pathway. Thus, the early response to TNF stimulation is activation of DAPK, which functions to prevent cells from initiating apoptosis unless they are subjected to strong or prolonged stimulation. During a strong or prolonged apoptotic stimulus, the extent

of degradation of DAPK varies depending on the rate of DAPK synthesis to alter the balance between survival and apoptosis.

Previous studies have identified two alternatively spliced isoforms of mouse DAPK (DAPK-α and DAPK-β) (2). These alternatively spliced forms of DAPK are identical in sequence except for 12 residues (RDSHAWTPLYDL) that extend the carboxyl terminus of DAPK-β. Characterization of these two forms of mouse DAPK using overexpression and antisense depletion studies has shown that mouse DAPK-α does not promote apoptosis and DAPK-β attenuates TNF-induced apoptosis (7). This issue has called into question the relevance of studies utilizing the mouse DAPK isoforms and has led to the suggestion that mouse DAPK is functionally different from human DAPK (36). In this study, the existence of an alternatively spliced form of human DAPK has been confirmed using RT-PCR and Western blotting. Comparison of the carboxyl-terminal mouse and human sequences reveals considerable sequence identity, and thus it is unlikely that there is a functional difference between mouse and human DAPK. In support of this proposal, antisense depletion of DAPK from primary human smooth muscle cells results in spontaneous, caspase-dependent apoptosis (7).

In summary, this report focuses on extending previous studies, suggesting that inhibitory autophosphorylation at Ser-308 of DAPK is important for modifying the catalytic activity of DAPK (14), and we have examined the mechanism by which the activities of DAPK are modulated in response to apoptotic stimulation. The results presented here show that DAPK undergoes a transient activation, is subsequently ubiquitinated, and then degraded by the proteasome. This paradigm is analogous to those that have been identified for temporally regulating other apoptosis/proliferation regulatory proteins such as p53 and retinoblastoma and may be a common mechanism used to rapidly modulate the activities of these important homeostatic factors (37,38). In addition to this mechanistic advance in our understanding of how the activities of DAPK are regulated, we have also confirmed the presence of an alternatively spliced human DAPK, denoted DAPK-β. This finding suggests that the functional differences identified in previous studies using mouse DAPK (7) are not because of species variations between mouse and human DAPK.

References

1. Deiss LP, Feinstein E, Berissi H, Cohen O, Kimchi A. Genes Dev 1995;9:15–30. [PubMed: 7828849]
2. Jin Y, Blue EK, Dixon S, Hou L, Wysolmerski RB, Gallagher PJ. J Biol Chem 2001;276:39667–39678. [PubMed: 11485996]
3. Cohen O, Inbal B, Kissil JL, Raveh T, Berissi H, Spivak-Kroizaman T, Feinstein E, Kimchi A. J Cell Biol 1999;146:141–148. [PubMed: 10402466]
4. Raveh T, Droguett G, Horwitz MS, DePinho RA, Kimchi A. Nat Cell Biol 2001;3:1–7. [PubMed: 11146619]
5. Pelled D, Raveh T, Riebeling C, Fridkin M, Berissi H, Futerman AH, Kimchi A. J Biol Chem 2002;277:1957–1961. [PubMed: 11709549]
6. Yamamoto M, Hioki T, Ishii T, Nakajima-Iijima S, Uchino S. Eur J Biochem 2002;269:139–147. [PubMed: 11784307]
7. Jin Y, Gallagher PJ. J Biol Chem 2003;278:51587–51593. [PubMed: 14530257]
8. Chen CH, Wang WJ, Kuo JC, Tsai HC, Lin JR, Chang ZF, Chen RH. EMBO J 2005;24:294–304. [PubMed: 15616583]
9. Cohen O, Feinstein E, Kimchi A. EMBO J 1997;16:998–1008. [PubMed: 9118961]
10. Kishino M, Yukawa K, Hoshino K, Kimura A, Shirasawa N, Otani H, Tanaka T, Owada-Makabe K, Tsubota Y, Maeda M, Ichinose M, Takeda K, Akira S, Mune M. J Am Soc Nephrol 2004;15:1826–1834. [PubMed: 15213270]

11. Yukawa K, Hoshino K, Kishino M, Mune M, Shirasawa N, Kimura A, Tsubota Y, Owada-Makabe K, Tanaka T, Ichinose M, Maeda M, Takeda K, Akira S. Int J Mol Med 2004;13:515–520. [PubMed: 15010850]
12. Yukawa K, Hoshino K, Kishino M, Tsubota Y, Owada-Makabe K, Maeda M, Bai T, Tanaka T, Akira S. Int J Mol Med 2005;16:389–393. [PubMed: 16077944]
13. Yukawa K, Kishino M, Hoshino K, Shirasawa N, Kimura A, Tsubota Y, Owada-Makabe K, Bai T, Tanaka T, Ueyama T, Ichinose M, Takeda K, Akira S, Maeda M. Int J Mol Med 2005;15:73–78. [PubMed: 15583830]
14. Shohat G, Spivak-Kroizman T, Cohen O, Bialik S, Shani G, Berrisi H, Eisenstein M, Kimchi A. J Biol Chem 2001;276:47460–47467. [PubMed: 11579085]
15. Kamm KE, Stull JT. J Biol Chem 2001;276:4527–4530. [PubMed: 11096123]
16. Zhi G, Abdullah SM, Stull JT. J Biol Chem 1998;273:8951–8957. [PubMed: 9535879]
17. Jin Y, Blue EK, Dixon S, Shao Z, Gallagher PJ. J Biol Chem 2002;277:46980–46986. [PubMed: 12351649]
18. Itoh M, Kim CH, Palardy G, Oda T, Jiang YJ, Maust D, Yeo SY, Lorick K, Wright GJ, Ariza-McNaughton L, Weissman AM, Lewis J, Chandrasekharappa SC, Chitnis AB. Dev Cell 2003;4:67–82. [PubMed: 12530964]
19. Citri A, Harari D, Shohat G, Ramakrishnan P, Gan J, Lavi S, Eisenstein M, Kimchi A, Wallach D, Pietrokovski S, Yarden Y. J Biol Chem 2006;281:14361–14369. [PubMed: 16551624]
20. Bai T, Tanaka T, Yukawa K, Maeda M, Umesaki N. Oncol Rep 2004;11:661–665. [PubMed: 14767518]
21. Friedrich MG, Weisenberger DJ, Cheng JC, Chandrasoma S, Siegmund KD, Gonzalgo ML, Toma MI, Huland H, Yoo C, Tsai YC, Nichols PW, Bochner BH, Jones PA, Liang G. Clin Cancer Res 2004;10:7457–7465. [PubMed: 15569975]
22. Kim WS, Son HJ, Park JO, Song SY, Park C. Int J Mol Med 2003;12:827–830. [PubMed: 14612952]
23. Narayan G, Arias-Pulido H, Koul S, Vargas H, Zhang FF, Villella J, Schneider A, Terry MB, Mansukhani M, Murty VV. Mol Cancer 2003;2:24. [PubMed: 12773202]
24. Li J, El-Naggar A, Mao L. Cancer 2005;104:771–776. [PubMed: 15959912]
25. Reddy AN, Jiang WW, Kim M, Benoit N, Taylor R, Clinger J, Sidransky D, Califano JA. Cancer Res 2003;63:7694–7698. [PubMed: 14633692]
26. Schildhaus HU, Krockel I, Lippert H, Malfertheiner P, Roessner A, Schneider-Stock R. Int J Oncol 2005;26:1493–1500. [PubMed: 15870861]
27. Tereshko V, Teplova M, Brunzelle J, Watterson DM, Egli M. Nat Struct Biol 2001;8:899–907. [PubMed: 11573098]
28. Foghsgaard L, Wissing D, Mauch D, Lademann U, Bastholm L, Boes M, Elling F, Leist M, Jaattela M. J Cell Biol 2001;153:999–1010. [PubMed: 11381085]
29. Foghsgaard L, Lademann U, Wissing D, Poulsen B, Jaattela M. J Biol Chem 2002;277:39499–39506. [PubMed: 12185082]
30. Guicciardi ME, Miyoshi H, Bronk SF, Gores GJ. Am J Pathol 2001;159:2045–2054. [PubMed: 11733355]
31. Chalfant CE, Kishikawa K, Mumby MC, Kamibayashi C, Bielawska A, Hannun YA. J Biol Chem 1999;274:20313–20317. [PubMed: 10400653]
32. Kishikawa K, Chalfant CE, Perry DK, Bielawska A, Hannun YA. J Biol Chem 1999;274:21335–21341. [PubMed: 10409693]
33. Chalfant CE, Szulc Z, Roddy P, Bielawska A, Hannun YA. J Lipid Res 2004;45:496–506. [PubMed: 14657198]
34. Shamloo M, Soriano L, Wieloch T, Nikolich K, Urfer R, Oksenberg D. J Biol Chem 2005;280:42290–42299. [PubMed: 16204252]
35. Henshall DC, Araki T, Schindler CK, Shinoda S, Lan JQ, Simon RP. J Neurochem 2003;86:1260–1270. [PubMed: 12911633]
36. Bialik S, Kimchi A. Annu Rev Biochem 2006;75:189–210. [PubMed: 16756490]
37. Shimizu H, Saliba D, Wallace M, Finlan L, Langridge-Smith PR, Hupp TR. Biochem J 2006;397:355–367. [PubMed: 16579792]

38. Ying H, Xiao ZX. Cell Cycle 2006;5:506–508. [PubMed: 16552188]

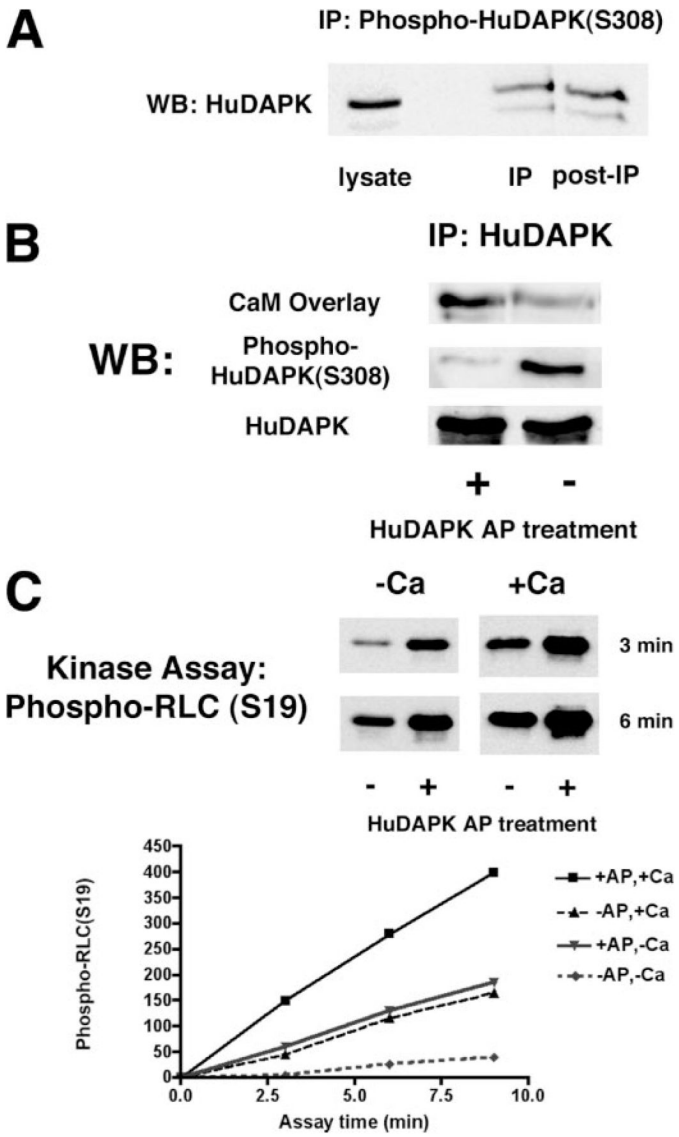

FIGURE 1. DAPK dephosphorylated at Ser-308 has increased kinase activity

A, Western blotting (*WB*) to detect immunoprecipitated (*IP*) phospho-DAPK and the level of unphosphorylated DAPK remaining in the supernatant following immuno-depletion of phospho-DAPK. Phosphorylated human DAPK (HuDAPK) from HeLa cells was immunoprecipitated with an antibody specific for DAPK phosphorylated at Ser-308; Western blotting was performed using a DAPK-specific antibody that detects both phospho-DAPK and unphosphorylated DAPK. *B*, Western blotting and CaM overlay of immunoprecipitated endogenous human DAPK treated with AP. The CaM overlay was carried out using biotinylated CaM (100 nM) in Tris buffer containing 10 mM Ca^{2+}. *C*, endogenous human DAPK was immunoprecipitated from HeLa cells. Immunoprecipitates were treated with AP to dephosphorylate the DAPK or with vehicle as a control. The kinase activity of the immunoprecipitates was then determined using myosin II RLC as a substrate in either the presence or absence of 600 μM Ca^{2+}. Western blots shown are representative of at least three independent analyses. Kinase assays were repeated at least three times.

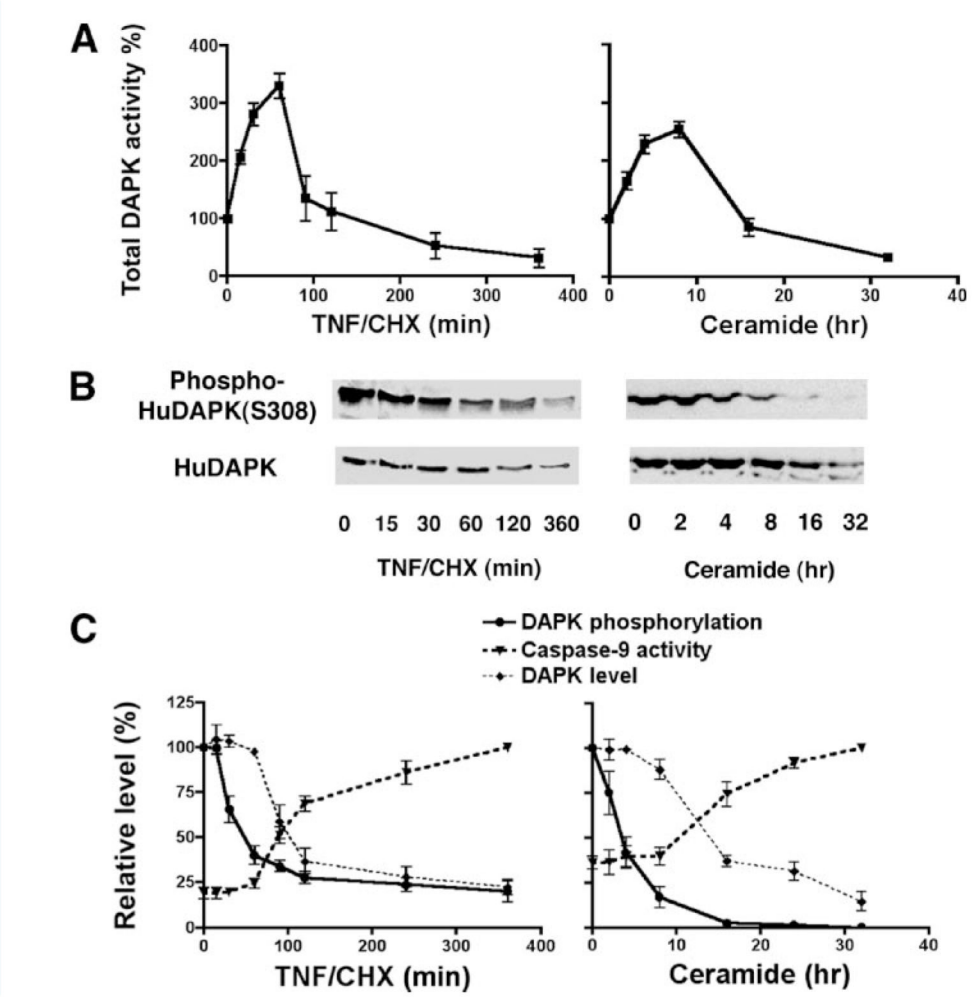

FIGURE 2. DAPK activity during TNF- or ceramide-induced apoptosis

A, kinase activity assay of immunoprecipitated total human DAPK from HeLa cells treated either with TNF (10 ng/ml)/cycloheximide (CHX, 10 μg/ml) or C_6-ceramide (50 μM) for the indicated times, using myosin II RLC as substrate. *B*, Western blotting of total human DAPK (HuDAPK) and DAPK phosphorylated at Ser-308 in HeLa cells treated either with TNF (10 ng/ml)/CHX (10 μg/ml) or C_6-ceramide (50 μM). *C*, graphs showing the relationship between the levels of human total DAPK, phospho-DAPK, and caspase-9 activity in HeLa cells treated with either TNF (10 ng/ml)/CHX (10 μg/ml) or ceramide (50 μM). The level of phosphorylated DAPK is normalized to the level of total DAPK at each time point. All experiments were repeated at least three times.

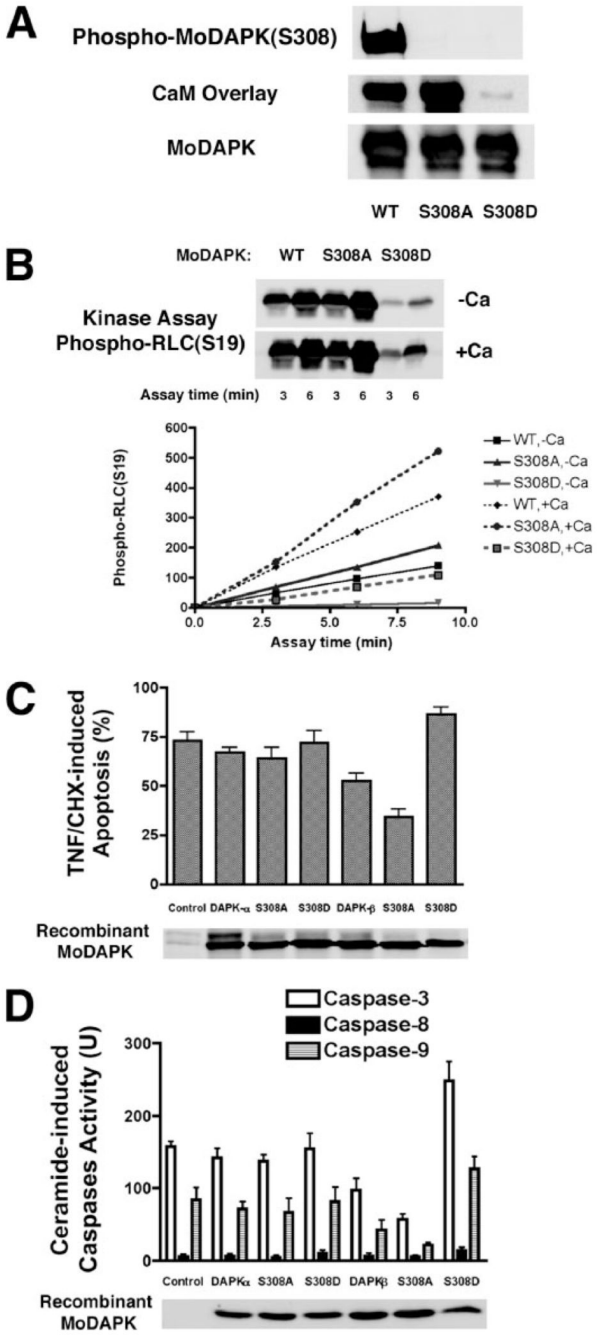

FIGURE 3. DAPK lacking an autophosphorylation site (S308A) has higher kinase activity and antagonizes apoptosis in HeLa cells treated with TNF or ceramide

A, Western blotting and calmodulin overlay of recombinant wild type (*WT*) or mutant (S308A or S308D) mouse DAPK-*α* that was transiently overexpressed and immunoprecipitated from HeLa cells. The calmodulin overlay binding assay was performed using biotinylated CaM incubated with a Western blot of the immunoprecipitated DAPK. *B*, kinase assay of recombinant wild type or mutant (S308A or S308D) mouse DAPK-*α* (*MoDAPK*) that was transiently overexpressed and immunoprecipitated from HeLa cells. Myosin II RLC was used as a substrate in the assay. The phosphorylated RLC (*phospho-RLC*) was detected using antibody specific for RLC phosphorylated at Ser-19. *C*, determination of TNF-induced

apoptosis in HeLa cells cotransfected with recombinant wild type mouse DAPK-α or DAPK-β or their mutant forms (S308A or S308D) together with LacZ in a ratio of 5 to 1. At 24 h after transfection, cell extracts were analyzed by Western blotting to detect the Omni-tagged recombinant mouse DAPK. Transfected HeLa cells were treated with TNF (10 ng/ml) and CHX (10 μg/ml) for 4 h before being fixed and stained to detect LacZ-positive cells. Transfected, LacZ-positive cells were scored as either apoptotic or normal based on morphology after LacZ staining. Control cells were cotransfected with luciferase and LacZ. A minimum of 100 cells was counted for each analysis in three independent transfections. *D*, determination of caspase-3, caspase-8, and caspase-9 activities in HeLa cells cotransfected with recombinant wild type mouse DAPK-α or DAPK-β or their mutant forms (S308A or S308D) together with GFP in a ratio of 5 to 1. At 24 h after transfection, fluorescence-activated cell sorter-enriched GFP-positive cells were Western-blotted for recombinant DAPK. Enriched cells were treated with ceramide (50 μM) for 24 h; cell extracts were prepared, and then analyzed to quantify caspase activities using synthetic peptide substrates in a colorimetric assay. Results are from three separate caspase assays from three independent transfections.

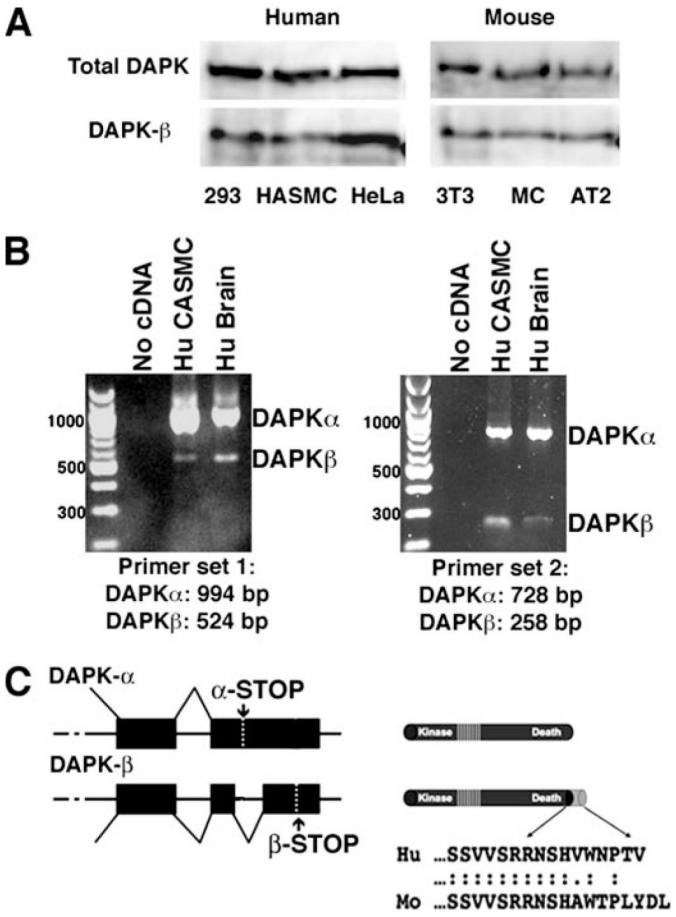

FIGURE 4. Identification of an alternatively spliced human DAPK

A, Western blotting of human and mouse cell line whole cell lysates using an antibody that recognizes total DAPK (*total DAPK*) or an antibody raised against the 12 carboxyl-terminal residues (RDSHAWTPLYDL) that are unique for mouse DAPK-*β* (2). *B*, reverse transcription PCR using primers designed to amplify the carboxyl terminus of both DAPK-*α* and DAPK-*β* detects both splice variants in human brain and HCASMC cDNAs. *HASMC*, primary human aortic smooth muscle cells; *MC*, primary mouse cardiomyocytes; *Hu CASMC*, primary human (*Hu*) coronary artery smooth muscle cells. *C*, schematic representation of the predicted DAPK-*α* and DAPK-*β* 3′ alternative splicing (*left*) and protein structure (*right*). DAPK-*β* uses an alternative splice site within the 3′-untranslated region of DAPK-*α*, which results in deletion of 477 bp of the DAPK-*α* and skips the DAPK-*α* stop codon (*α-STOP*). Use of this alternative splice site results in addition of 10 additional residues and utilizes the DAPK-*β* stop codon (*β-STOP*). Cloning and sequencing of the PCR products verified the DAPK-*α* and DAPK-*β* carboxyl-terminal sequences, shown below the protein schematic at the *right side*.

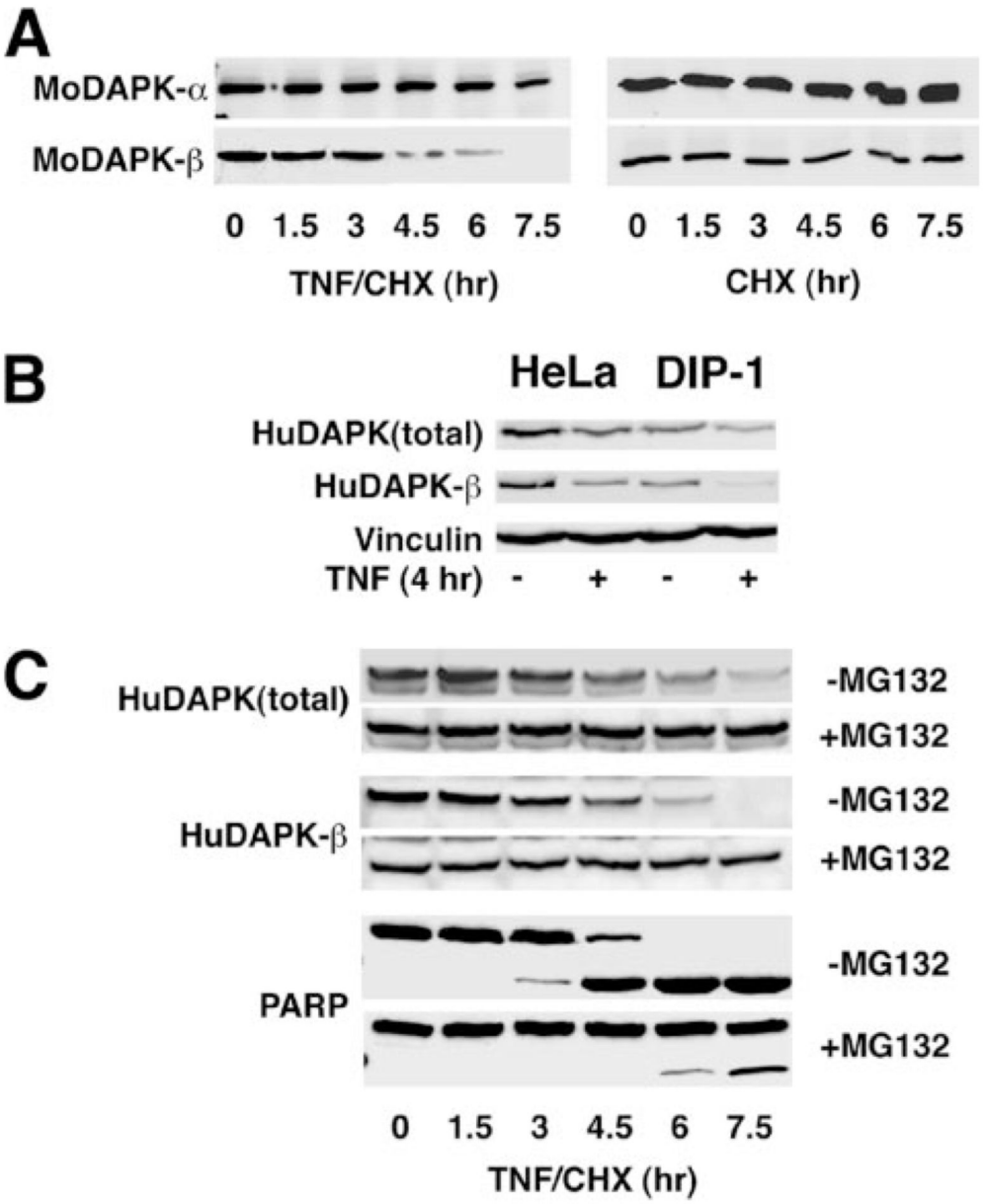

FIGURE 5. DAPK is degraded by proteasomal activity during TNF-induced apoptosis

A, Western blotting of recombinant mouse DAPK-*α* (*MoDAPK-α*) and DAPK-*β* (*MoDAPK-β*) in HeLa cell lines treated with either TNF (10 ng/ml) and CHX (10 *μ*g/ml) or CHX (10 *μ*g/ml) alone for the indicated times. *B*, Western blotting of endogenous human DAPK-*β* (*HuDAPK*) in HeLa cells or HeLa cells overexpressing the ubiquitin E3 ligase DIP-1 treated with TNF (10 ng/ml) or vehicle. Western blotting to detect vinculin was used to control for equal sample loading. *C*, Western blotting of endogenous human DAPK-*β* in HeLa cells treated with TNF (10 ng/ml) and CHX (10 *μ*g/ml) for indicated time, in the presence or absence of MG132 (50 *μ*M), a proteasome inhibitor. Also shown is a Western blot of PARP, cleavage of which is used as an indicator of caspase activation.